

Electron-Stimulated-Desorption Ion Angular Distributions of Negative Ions

Allen L. Johnson,^(a) Stephen A. Joyce, and Theodore E. Madey^(b)

National Institute of Standards and Technology (formerly National Bureau of Standards), Gaithersburg, Maryland 20899

(Received 22 June 1988)

We report the first measurements of the electron-stimulated-desorption ion-angular-distributions of negative ions from surfaces. The angular distributions of F^- ions for electron-stimulated desorption of PF_3 , NF_3 , and $(CF_3)_2CO$ on Ru(0001) depend on the molecular geometry and the state of the adsorbed species. The structural information obtained from these negative-ion studies complements that from similar positive-ion studies.

PACS numbers: 61.14.Ki, 79.20.Kz, 82.65.My

Electron-stimulated-desorption ion angular distributions (ESDIAD) of positive ions is a highly useful tool for determining the bonding structure of atoms and molecules adsorbed on single-crystal surfaces.¹ This is because the direction of ion desorption from the surface is determined by the orientation of the bond which is ruptured by electron bombardment. In addition to positive ions, electron-stimulated desorption (ESD) of adsorbed species also causes desorption of neutral products (atoms and molecules) as well as negative ions.² The relative yields of positive ions, negative ions, and neutral species vary depending on the molecule, the bonding geometry, molecular coverage, etc.

Whereas ESD angular distributions of both positive ions^{1,3} and neutral species^{4,5} have been reported previously, we describe here the first measurements of ESD angular distributions of negative ions. We report data for F^- ESDIAD from several fluorine-containing molecules adsorbed on Ru(0001) at 110 K, for which high yields of both F^- and F^+ ions are seen. The negative ions originate mainly from parent molecular adsorbates, while the positive-ion yield is higher for adsorbed dissociation fragments. There is striking angular anisotropy observed in negative-ion ESDIAD, providing structural information complementary to that derived from positive-ion ESDIAD. The comparison of ESDIAD data for F^+ and F^- also provides insights into the ion formation mechanisms.

For these studies, we have chosen three molecules [PF_3 , NF_3 , and $(CF_3)_2CO$] known to yield F^- ions upon electron impact in the gas phase.^{6,7} Adsorption studies of

these molecules have been conducted on the Ru(0001) surface.⁸⁻¹⁰

The major technical challenge in negative-ion ESDIAD is to separate the large secondary electron signal from the much weaker (by approximately 10^{-4}) negative-ion signal. We accomplish this by using time-of-flight techniques in an electrostatic mirror time-of-flight apparatus¹¹ adapted from the existing digital ESDIAD apparatus.^{1,12} Typical electron bombardment energies are ~ 280 eV, with use of a pulsed electron beam (repetition rate $\sim 10^4/s$). Under typical conditions, the electron flight time is < 30 ns and the flight time for an F^- ion is ~ 99 ns. This experimental apparatus can be used for mass-resolved positive-ion studies as well.

For all of the systems studied [PF_3 , NF_3 , and $(CF_3)_2CO$] both the positive- and negative-ion ESDIAD are dominated by fluorine ion emission. The observed yields for F^+ and F^- ESDIAD for the systems studied are summarized in Table I. We observe that the total angle integrated F^- yields from these fluorinated molecules are a significant fraction of the total ($F^+ + F^-$) ion current [from 3% for NF_3 to 40% for monolayer $(CF_3)_2CO$, to 80% for multilayers of $(CF_3)_2CO$].

Strong angular anisotropies in the F^- emission are observed. Figure 1 shows patterns seen for annealed ($T \sim 270$ K) overlayers of PF_3 , NF_3 , and $(CF_3)_2CO$ on Ru(0001). Beams are seen along the surface normal for all these systems, and for PF_3 and $(CF_3)_2CO$ hexagonally symmetric patterns are seen after annealing. The ESDIAD patterns are clearly dependent on the molecular species and its chemical state.

TABLE I. Ion yields (ions/electron) of saturation coverage adlayers on Ru(0001). Electron impact energy is 280 eV; $T_s \approx 110$ K. Yields are angle integrated over the entire ESDIAD image.

	F^+ yields	F^- yields	$F^-/(F^- + F^+)$
PF_3	3×10^{-6}	2×10^{-7}	0.08
NF_3	4×10^{-7}	1×10^{-8}	0.03
$(CF_3)_2CO$	8×10^{-7}	6×10^{-7}	0.43
$(CF_3)_2CO$ (multilayer)	1×10^{-6}	6×10^{-6}	0.83

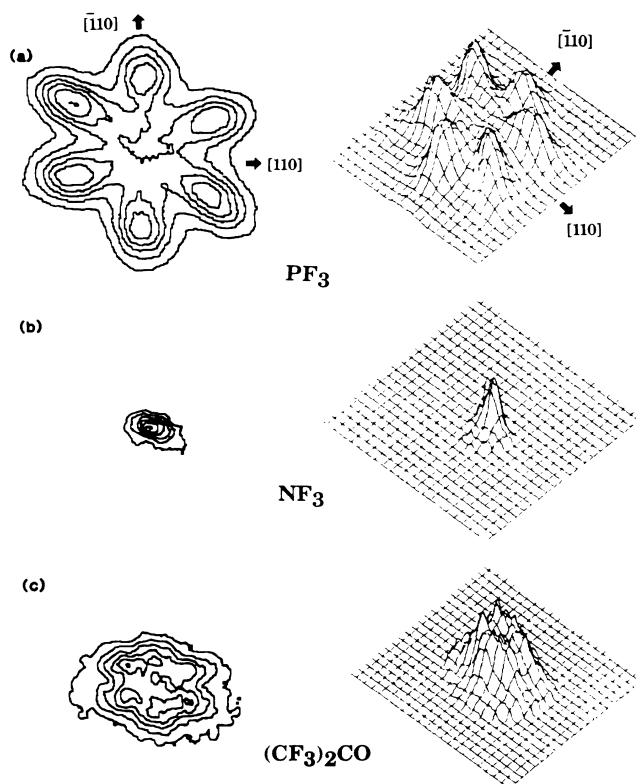


FIG. 1. F^- ESDIAD for (a) PF_3 , (b) NF_3 , and (c) $(CF_3)_2CO$ on Ru. All of these samples have been dosed to saturation at 110 K and annealed to temperatures of 140–270 K. On the left are contour plots of ion signal; on the right are the corresponding perspective plots. [The asymmetries on the right sides of (a) and (c) are due to variations in gain across the microchannel plates.]

Another general observation for all three adsorbed molecules is that the negative-ion signal invariably *decreases* with electron beam exposure (due to beam damage), while the positive-ion signal *increases*. This is consistent with the generation of negative ions from parent molecular species, while the positive ions have a high probability of production from surface fragments as well as molecular adsorbates. The dominance of positive-ion emission from fragment and minority species for certain adsorbates has been noted,¹³ and can complicate the interpretation of the ESDIAD results.

A discussion of the comparative surface chemistry and ESDIAD behavior for all of these adsorbates is outside the scope of this Letter; rather, this Letter focuses in detail on PF_3 on Ru(0001) as an example of the utility of negative-ion ESDIAD. These measurements provide new insights into the structure of adsorbed PF_3 , not observable from positive-ion ESDIAD.

Figure 2 shows the temperature-dependent ESDIAD yields (angle resolved) and the thermal desorption spectra (TDS) of a saturation coverage of PF_3 on Ru(0001). This illustrates another systematic trend observed for all

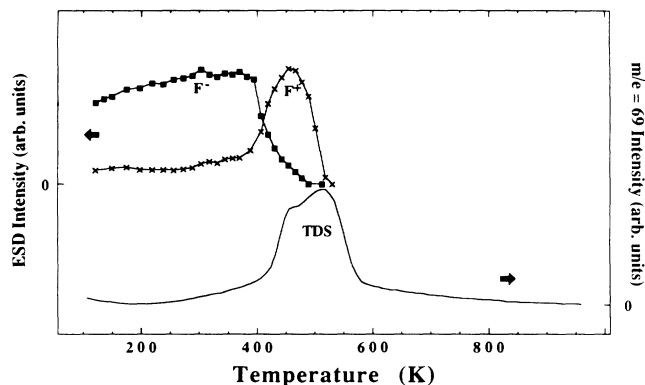


FIG. 2. Temperature dependence of the F^+ , F^- , and molecular desorption of PF_3 from Ru(0001). The heating rate was ~ 10 K/s. The ion signals correspond to the peak intensities of the off-normal emission.

three adsorbates studied, i.e., the negative-ion signal decreases on moderate warming whereas the positive-ion signal either stays the same or increases. The increase in intensity of F^+ emission upon heating in the case of PF_3 on Ru(0001) occurs only when the coverage is high, and seems to be associated with the thermal decomposition of PF_3 to form PF_2 and PF fragments, similar to what is seen in the electron-beam-induced decomposition of PF_3 on Ni(111),¹⁴ and in the beam damage experiments described above. The shoulder in the TDS peak at lower temperatures is a reproducible feature that appears only with PF_3 coverages above 0.75 of saturation. The tracking of the negative-ion signal with the low-temperature component of the molecular TDS peak, and the loss of positive-ion signal at higher temperature is further evidence that the negative ions originate mainly from molecular surface species, while the positive ions originate from surface fragments as well as molecular adsorbates.

The ESDIAD of a saturation coverage of PF_3 on Ru(0001) dosed at 110 K shows changes as a function of temperature in the ion angular distributions that are different for F^+ and F^- (Fig. 3). Before annealing [Figs. 3(a) and 3(c)], PF_3 exhibits a broad emission maximum along the surface normal in F^- ESDIAD, but little normal emission and maxima along six beams inclined with respect to the surface normal in F^+ ESDIAD. After annealing to ~ 270 K [Figs. 3(b) and 3(d)], the F^- ESDIAD shows maxima along six beams inclined with respect to the surface normal, while the F^+ ESDIAD exhibits both normal and off-normal emission (which we believe is due to thermally generated PF_2 and PF). These differences are characteristic of changes in the surface state of the PF_3 .

The data of Figs. 2 and 3 have implications for the mechanism of ion formation as well as for the structural aspects of PF_3 on Ru(0001), and we discuss these topics

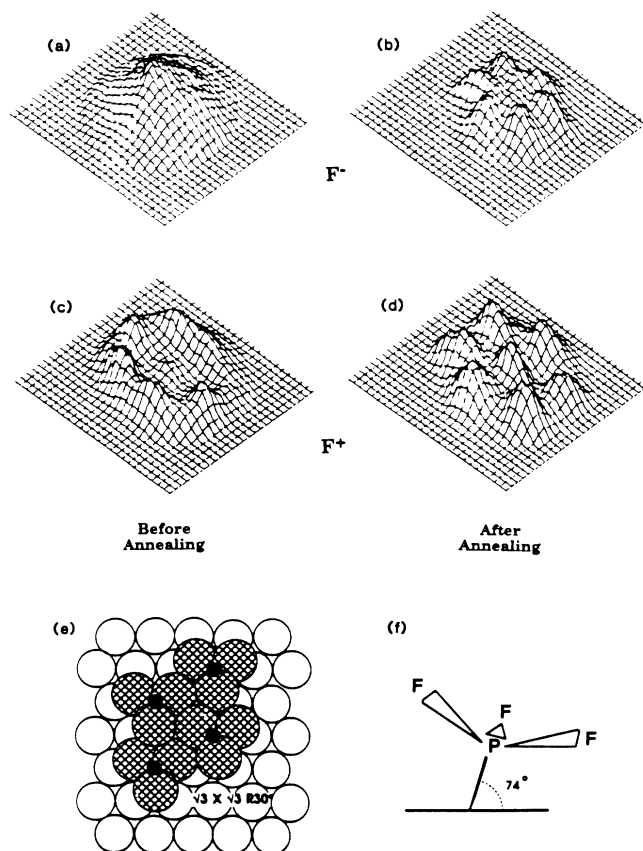


FIG. 3. Comparison of the (a), (b) F^- and (c), (d) F^+ ES-DIAD of PF_3 on Ru(0001), before (a) and (c) and after (b) and (d) annealing to $T \sim 270$ K. These results were obtained from a single adsorbate sample. Notice the rotation of the F^+ emission beams by 30° from along Ru atom rows in (c) to between Ru rows in (d) (Ref. 17). Models of the PF_3 high coverage state: (e) Lattice model drawn to scale. (f) Bonding model for the proposed tilted PF_3 state.

in turn.

In the gas phase^{6,7} and in physisorbed layers,² negative ions are produced via several different mechanisms, including dissociative attachment and dipolar dissociation, which generally involve populating of the antibonding levels in the molecule. On surfaces, positive ions can also charge exchange to produce a negative-ion flux; almost complete charge conversion ("harpooning") has been observed in ion-scattering experiments.¹⁵

In the charge-exchange (harpooning) mechanism, the negative-ion yield is due to a charge transfer from the highest occupied substrate orbitals to an outgoing positive ion; the reneutralization rate of a negative ion is, in turn, limited by charge transfer to the lowest unoccupied surface orbitals. Depending on the symmetries of both the occupied and unoccupied states, the angular dependencies of F^- and F^+ ES-DIAD could be similar. As

shown in Figs. 2 and 3 the differences in F^+ and F^- ES-DIAD for PF_3 on Ru(0001) are considerable for different coverages and temperatures. However, the differences in the angular anisotropies seen in Fig. 3 are complicated by the effects of image charges and reneutralization of the ions.¹⁶ The F^- ions desorb with lower kinetic energy than the F^+ ions, which may lead to the capture of the off-normal beams. The simplest way to demonstrate that the angular distribution is different for F^+ and F^- is to examine the behavior of the normal emission beam. The clear differences in the intensity and temperature dependence of the normal emission (Fig. 3) lead us to suggest that the harpooning mechanism is not dominant in these systems.

Either the dissociative attachment or dipolar dissociation mechanism can account for the observed chemical specificity for negative-ion emission. The negative-ion yield is controlled by the lifetime of the electron in a relatively large antibonding orbital (in contrast to the positive-ion production which involves deep valence excitations and core holes); the lifetime of the antibonding state is expected to be shorter for the covalently bonded fragments than for the chemisorbed parent molecules. The dissociative attachment process is expected to have a resonance at ~ 2.2 eV, while dipolar dissociation should have a higher energy threshold (at ~ 12 eV).⁷ The threshold measurements needed to distinguish between these mechanisms are currently under way.

Consider now the structure of adsorbed PF_3 . For less than saturation coverage, the PF_3 F^+ ES-DIAD pattern is found to be an azimuthally disordered halo, with the F^+ emission at $\sim 70^\circ$ from the surface normal.¹⁷ The adlayer thermally desorbs reversibly, with no change in the ES-DIAD pattern and no decomposition. In contrast to earlier ES-DIAD studies of PF_3 on Ni(111) (Ref. 14) no discernable evidence for hindered rotation at low coverages at our lowest temperature, 110 K, is observed. This is in marked contrast to the results at higher coverages, where azimuthal ordering of PF_3 occurs [Fig. 3(c)].¹⁷

For saturation coverage of PF_3 a tilted, compressed state is proposed, based on a number of observations. The polar angle of the F^+ halo under field-free conditions is 70° , while the F^- "flower" pattern [Figs. 1(a) and 3(b)] polar angle is 50° . The ion energies and angles are such that we do not attempt to correlate quantitatively the polar angle with bond angle, but the lower energy of the negative ions suggests that the F^- emission direction must have a smaller polar angle than the corresponding F^+ signal at the surface, since the lower energy ion will be bent *further* from the surface normal as a result of the effects of the image charge.¹⁶ However, the F^- beam is observed *closer* to the normal than the F^+ beam [compare Figs. 3(b) and 3(d)].

Further, one notices that the beam profiles of the F^- flower pattern [Fig 1(a)] are broader in the polar angle

than in the azimuthal angle. Although various factors contribute to ESDIAD beam widths, this observation is consistent with a model in which the P-F motions in polar angle are more facile than for the azimuthal angle. This beam profile is not observed in the hexagonal F^+ ESDIAD pattern [Fig. 3(d)] which is due to ion emission from thermally generated PF_2 .¹⁷

Lastly, the formation of the F^- flower pattern occurs simultaneously with the formation of a $(\sqrt{3} \times \sqrt{3})R30^\circ$ low-energy electron diffraction pattern. This LEED pattern is seen only when the surface is dosed to above 0.5 of saturation, the coverage where the low-temperature shoulder on the PF_3 TDS develops. The unit cell implied by this pattern, assuming the PF_3 molecular axis is normal and with use of PF_3 geometrical parameters derived from coordination chemistry,^{18,19} gives an approximately 0.1-Å overlap of the fluorine van der Waals radii [Fig. 3(e)].

These facts lead us to propose that the PF_3 in the high coverage state is tilted, with the molecular axis tilted approximately 16° from the surface normal [Fig. 3(f)]. This tilt is sufficient to remove the overlap and to bring the fluorine van der Waals radii of adjacent PF_3 units into contact. Further, such a tilt is consistent with the observed smaller polar angle for the PF_3 F^- ESDIAD pattern in comparison with the F^+ ESDIAD pattern.

In summary, the results of the first negative-ion ESDIAD investigations of PF_3 , NF_3 , and $(CF_3)_2CO$ on Ru(0002) are reported. In all of these systems large yields of F^+ and F^- are observed. The negative-ion yield is dominated by molecular adsorbates, whereas the positive-ion yield is higher for dissociation fragments. Negative-ion ESDIAD provides structural information that complements the information derived from positive-ion ESDIAD. We have demonstrated this with the results of our investigation of PF_3 on Ru(0001) which shows the existence of a high coverage, compressed, tilted adsorption state. The chemical specificity and differential behavior of the positive- and negative-ion ESDIAD patterns show that the charge conversion ("harpooning") mechanism for negative-ion production on surfaces is not dominant in the system studied.

Partial support for this work was provided by the Department of Energy, Office of Basic Energy Sciences and a joint National Bureau of Standards-National

Research Council Research grant. The authors acknowledge valuable discussions with Dr. J. W. Gadzuk and Dr. D. E. Ramaker.

^(a)Present address: Surface Science Centre, University of Liverpool, Liverpool L69 3BX, United Kingdom.

^(b)Present address: Serin Physics Laboratory, Rutgers, The State University, Piscataway, NJ 08854.

¹T. E. Madey, *Science* **234**, 316 (1986).

²R. Azria, L. Parenteau, and L. Sanche, *J. Chem. Phys.* **88**, 5166 (1988).

³J. J. Czyzewski, T. E. Madey, and J. T. Yates, Jr., *Phys. Rev. Lett.* **32**, 777 (1974).

⁴P. Feulner, in *Proceedings of DIET II*, edited by W. Brenig and D. Menzel, Springer Series in Surface Sciences Vol. 4 (Springer-Verlag, New York, 1985) p. 142.

⁵M. D. Alvey, M. J. Dresser, and J. T. Yates, Jr., *Phys. Rev. Lett.* **56**, 367 (1986).

⁶J. G. Dillard, *Chem. Rev.* **73**, 589 (1973).

⁷D. F. Torgeson and J. B. Westmore, *Can. J. Chem.* **53**, 933 (1975).

⁸F. Nitschke, G. Ertl, and J. Küppers, *J. Chem. Phys.* **74**, 5911 (1981).

⁹M. M. Walczak, A. L. Johnson, P. A. Thiel, and T. E. Madey, *J. Vac. Sci. Technol. A* **6**, 675 (1988).

¹⁰M. M. Walczak, P. K. Leavitt, and P. A. Thiel, *J. Am. Chem. Soc.* **109**, 5621 (1987).

¹¹A. L. Johnson, S. A. Joyce, and T. E. Madey, to be published.

¹²A. L. Johnson, R. Stockbauer, D. Barak, and T. E. Madey, in *Proceedings of DIET-III*, edited by M. Knotek and R. Stulen, Springer Series in Surface Sciences (Springer-Verlag, New York, to be published).

¹³T. E. Madey, M. Polak, A. L. Johnson, and M. M. Walczak, in Ref. 12.

¹⁴M. D. Alvey, J. T. Yates, Jr., and K. J. Uram, *J. Chem. Phys.* **87**, 7221 (1987); M. D. Alvey and J. T. Yates, Jr., *J. Chem. Soc.* **110**, 1782 (1988).

¹⁵J. J. C. Geerlings, P. W. Van Amersfoort, L. F. Tz. Kwakman, E. H. A. Granneman, J. Los, and J. P. Guyacq, *Surf. Sci.* **157**, 151 (1985).

¹⁶Z. Miskovic, J. Vukanic, and T. E. Madey, *Surf. Sci.* **169**, 405 (1986).

¹⁷S. A. Joyce, A. L. Johnson, and T. E. Madey, to be published.

¹⁸L. Malatesta and S. Cenini, *Zerivalent Compounds of Metals* (Academic, London, 1974), p. 97.

¹⁹A. Bondi, *J. Phys. Chem.* **68**, 441 (1964).